Available online at www.sciencedirect.com
ScienceDirect
Journal of Sound and Vibration 321 (2009) 631–646
JOURNAL OF SOUND AND VIBRATION
www.elsevier.com/locate/jsvi

Resonance frequencies of parallelepipeds for determination of elastic moduli: An accurate numerical treatment

J.I. Etcheverry*, G.A. Sánchez

Applied Physics Department, Center for Industrial Research, TenarisSiderca, Dr. Simini 250 (B1804MHA) Campana, Buenos Aires, Argentina

Received 20 February 2008; received in revised form 28 October 2008; accepted 28 October 2008
Handling Editor: S. Bolton
Available online 16 December 2008

Abstract

The elastic resonance and impulse excitation of vibration are standard techniques to determine the elastic moduli of materials, with important applications to glass, metals, ceramics, rocks, etc. The validity of the analytical expressions used for prismatic bars is analyzed in detail in this work by numerically solving the three-dimensional linear elasticity equations, providing in particular error estimations for the formulae in ASTM standards. The results help to choose the sample dimensions, indicate which expressions are better to use in order to achieve some desired level of accuracy, and provide a means to correct the obtained results.

1. Introduction

The sonic resonance and impulse excitation of vibration techniques are well established and widely used techniques for the determination of the dynamic elastic properties of a large diversity of materials (steel, concrete, glass, ceramic, graphite, etc.). They are, in particular, covered by several ASTM standards, see, for example, E1875-00e1, E1876-07, C1548-02 [1–3]. The techniques consist in vibrating a sample by either applying a harmonic perturbation or exciting it with an impulse, and inferring the elastic moduli from the measured lowest resonance frequencies. They are quite appealing because they only require simple equipment, like an inexpensive microphone, if the sample dimensions are chosen in such a way that the resonances are in the audible range, and a PC with a standard sound card. Much more sophisticated analyses have been carried out using optical transducers to map the resonance modes [4], and more recently using laser interferometry to determine the shape of the resonance modes together with the resonance frequencies [5].

Similar techniques have been developed for cylindrical, square and rectangular bars, for spheres, disk shaped samples, etc. The simplicity of preparing prismatic bars does, however, make the particular case under analysis one of the preferred ones. Also important is the simplicity of the excitation and the detection of torsional modes, which is difficult in the case of cylindrical samples. As compared to other techniques to

*Corresponding author. Tel.: +54 3489 433100x35413; fax: +54 3489 427928.
E-mail addresses: jetcheverry@tenaris.com (J.I. Etcheverry), sidgsa@siderca.com (G.A. Sánchez).

0022-460X/$ - see front matter © 2008 Elsevier Ltd. All rights reserved.
doi:10.1016/j.jsv.2008.10.026

determine the elastic properties, both impact excitation of vibration and sonic resonance are highly repetitive, and provide accurate results [6]. This constitutes a strong motivation to improve the currently used analytical formulae in such a way that the full precision allowed by the technique can be achieved, and to assess the error involved in the several analytical expressions recommended by the standards.

The method in the simple form addressed here (and in the referenced ASTM standards) is adequate for linear elastic isotropic and homogeneous materials. Already some of the early references considered the more general problem of determining the resonance properties of piezoelectric ceramic rectangular parallelepipeds [7], cubes [8] and rectangular parallelepipeds with very general crystalline symmetries [9]. As they were based on numerical simulations and presented results for only a few cases which cannot be accurately interpolated, they did not provide the tools for a simple widely applicable technique.

For a linear elastic isotropic homogeneous prismatic bar, there are several analytical expressions that relate the elastic moduli to the flexural, torsional and longitudinal lowest resonance frequencies. They are usually obtained not directly from the three-dimensional (3-D) linear elasticity equations but from approximate theories [10]. These formulae have been tested against experimental data by several authors [11–13], leading in some cases to the proposal of empirical correction factors as in [12] for the fundamental torsional resonance. These are still commonly used (see for instance ASTM standards E1876-01, C1548-02 (2007), ASTM E1875-00e1) [1–3], although in the latest revision of ASTM standard E1876-07 they were replaced by the theoretical approximate expressions from [11]. Surprisingly, to authors' knowledge, there are no systematic comparisons between the analytical formulae and the results of the numerical solution of the 3-D elasticity equations. Some comparisons for particular conditions are presented for instance in [5].

In the early Refs. [7–9] there are quite successful attempts to solve the 3-D elastic problem with zero stress (Neumann) conditions by means of a variational formulation. They use a Galerkin approximation method: a simple 'p-version' finite element approach with a single element and a set of basis functions that are either trigonometric functions [7] or Legendre polynomials [8]. Due perhaps to limitations in computing power, however, the results are applied only to a few cases, and the expected error in the relevant frequencies is not small. In all cases they exploit the symmetry of the problem to simplify the calculations and identify the frequencies corresponding to each physical mode. Surprisingly, there is no explicit recognition of the fact that some of the resonance modes may be non-smooth [14], which degrades the accuracy of the corresponding solutions and eigenvalues. Comparison of the numerical eigenvalues with the theoretical Lamé solutions for a cube, as done in [8] is not enough, because these solutions are smooth. On a different approach, similar to the one applied to cylindrical bars, several authors developed techniques to approximate the displacements by means of series solutions [15,16].

In the following we implement a numerical solution of the 3-D elasticity equations, based on Legendre polynomials [8], and analyze numerically the precision of the obtained resonance frequencies. Once the precision of the results can be ascertained, we compare the numerical frequencies with those predicted by the available analytical expressions, and discuss their range of validity.

2. Numerical approach

The 3-D linear elasticity equations for a rectangular parallelepiped of dimensions L_x, L_y, L_z (it will be assumed in the rest of this paper that $L_x \geqslant L_y \geqslant L_z$) are

$$\mu\Delta\mathbf{u} + (\lambda+\mu)\nabla(\nabla\cdot\mathbf{u}) = \rho\frac{\partial^2\mathbf{u}}{\partial t^2} \quad \text{in } \Omega\times[0,T], \tag{1}$$

where $\mathbf{u}$ is the vector of displacements, λ, μ are the Lamé parameters, ρ is the density of the material, $\boldsymbol{\tau}$ is the stress tensor, $\Omega = [-L_x/2, L_x/2]\times[-L_y/2, L_y/2]\times[-L_z/2, L_z/2]$, T is the maximum time and $\mathbf{n}$ is the normal to the boundary.

The boundary conditions here are of zero stress (homogeneous Neumann conditions):

$$\boldsymbol{\tau}\mathbf{n}|_{\partial\Omega} = 0. \tag{2}$$

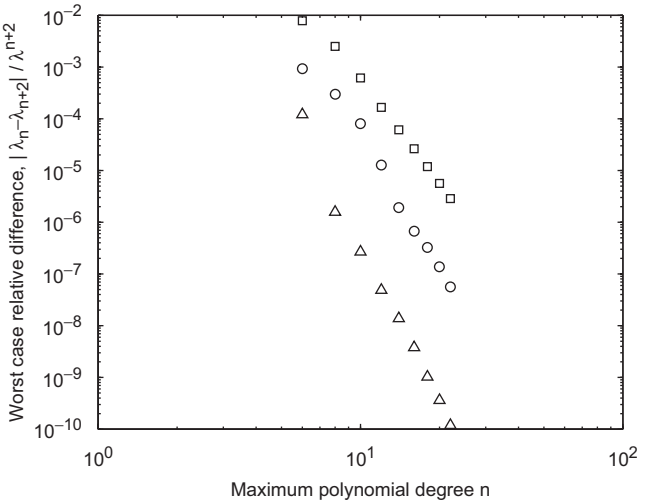

Fig. 1. Worst case (over the whole computational $40 \times 30 \times 9$ grid) relative difference between resonance frequencies computed for $n = 6$, 8, 10, 12, 14, 16, 18, 20, 22, 24, as a function of the maximum approximation degree n. Circles: flexural mode, squares: torsional mode, triangles: longitudinal mode.

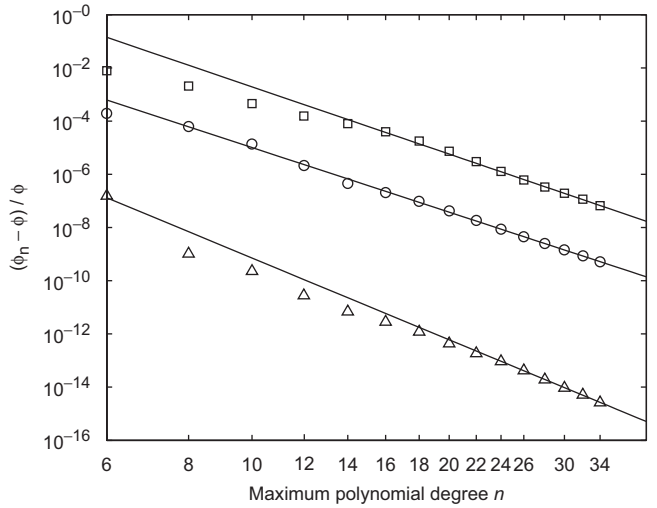

Fig. 2. Asymptotic behavior of the resonance frequencies vs. n for Poisson ratio $\nu = 0.3$, length-to-width equal to 5 and width-to-thickness equal to 10. Circles: flexural mode, squares: torsional mode, triangles: longitudinal mode. Solid lines correspond to best fits using Eq. (8).

The eigenvalue problem associated to Eq. (1) is

$$\mu\Delta\mathbf{u} + (\lambda + \mu)\nabla(\nabla \cdot \mathbf{u}) = -\rho\omega^2\mathbf{u} \quad \text{in } \Omega \tag{3}$$

with boundary conditions given by (2). Here ω is the angular frequency related to the resonance frequency f through $\omega = 2\pi f$. The standard variational formulation is obtained by taking the L^2 scalar product with a trial function $\boldsymbol{\phi} = (\phi_1, \phi_2, \phi_3)$ and integrating over the whole domain. Through the addition of a suitable volume integral and using the divergence theorem, the boundary terms can be brought to the form of an integral of the stresses on the surface, which are zero. In this way, all boundary terms vanish in the variational formulation, which constitutes an advantage over other methods (finite differences, collocation, etc.). The final

variational formulation is [17]

$$\lambda \int_\Omega (\nabla \cdot \mathbf{u})(\nabla \cdot \boldsymbol{\phi})\,\mathrm{d}\mathbf{x} + 2\mu \int_\Omega \sum_{i,j=1}^{3} \varepsilon_{ij}(\mathbf{u})\varepsilon_{ij}(\boldsymbol{\phi})\,\mathrm{d}\mathbf{x} = \rho\omega^2 \int_\Omega \mathbf{u}\cdot\boldsymbol{\phi}\,\mathrm{d}\mathbf{x} \tag{4}$$

for all $\mathbf{u}$, $\boldsymbol{\phi} \in \mathbf{H}^1(\Omega)$, where the strain tensor $\boldsymbol{\varepsilon}_{ij}(\mathbf{u})$ is given by

$$\varepsilon_{ij}(\mathbf{u}) = \varepsilon_{ji}(\mathbf{u}) = \frac{1}{2}\left(\frac{\partial u_i}{\partial x_j} + \frac{\partial u_j}{\partial x_i}\right). \tag{5}$$

The solution to this problem is approximated in the subspace of polynomials in x, y and z, of overall degree up to some maximum value n, leading to a finite dimension generalized eigenvalue problem of the form $\mathbf{K}\mathbf{v} = \alpha\mathbf{M}\mathbf{v}$, where $\mathbf{K}$ is the symmetric positive semi-definite stiffness matrix, and $\mathbf{M}$ is the mass matrix which is positive definite. This problem has six zero eigenvalues, which correspond to the six degrees of freedom of the rigid solid. The dimension of the approximation space is $(n+3)(n+2)(n+1)/2$ (cf. Eq. (6)). For some examples degrees up to $n = 34$ are used. Instead of using the monomials base $(1, x, y, z, x^2, y^2, z^2, xy, xz, yz, \ldots)$, we follow [8] and use products of Legendre polynomials of the form:

$$\mathbf{u}_{i,j,k,l}(x,y,z) = P_i\left(\frac{2x}{L_x}\right)P_j\left(\frac{2y}{L_y}\right)P_k\left(\frac{2z}{L_z}\right)\hat{\mathbf{x}}_l, \quad i+j+k \leqslant n, \;\; l = 1,2,3. \tag{6}$$

This is a sensible choice, because the orthogonality properties of Legendre polynomials make the mass matrix $\mathbf{M}$ diagonal and the stiffness matrix $\mathbf{K}$ very sparse. As the problem is invariant against reflections in the three axes, the solutions have symmetries that can be exploited. A full account can be found in [7–9]. Grouping the basis functions by their symmetry makes the stiffness matrix a matrix with eight blocks. These can be assembled and solved independently, thus reducing both the time and memory requirements for the computational solution. These computations were programmed in Matlab, both using the standard full matrix eigenvalue computation routines, or those to compute a few eigenvalues of a sparse matrix.

3. Numerical results

In order to analyze the validity range of available formulas for flexural, torsional and longitudinal vibration modes, the algebraic eigenvalue problem was solved for several approximation degrees, scanning a wide range of the problem parameters. It is obvious from a simple scaling argument that the problem has three independent parameters, which can be chosen as the length-to-width ratio, the width-to-thickness ratio, and the Poisson ratio. Changes in the remaining parameters (density ρ, length L_x and Lamé constant λ, for instance) simply lead to a rescaling of the obtained resonance angular frequencies. In particular, if the angular frequencies ω are computed using some given density, length and λ, but are sought for some different ρ', L_x', λ', they can be obtained as

$$\omega' = \frac{L_x}{L_x'}\sqrt{\frac{\rho}{\rho'}\frac{\lambda'}{\lambda}}\,\omega. \tag{7}$$

The same formula is of course valid for the corresponding frequencies f, f'. The values for L_x, ρ and λ assumed in the simulations below are given in Table 1, unless explicitly stated otherwise.

In the following the length-to-width ratio L_x/L_y is scanned from 1 to 15 in 40 logarithmically spaced steps, the width-to-thickness ratio L_y/L_z is scanned from 1 to 10 in 30 logarithmically spaced steps, and the Poisson ratio ν is scanned at 0.05 steps from 0.05 to 0.45. Logarithmically spaced partitions (equally spaced in the

Table 1
Values of the sample length, density and Lamé constant λ used in the simulations below, unless explicitly stated.

Parameter	L_x (m)	ρ (kg/m^3)	λ (GPa)
Value	0.09995	7812	111.15

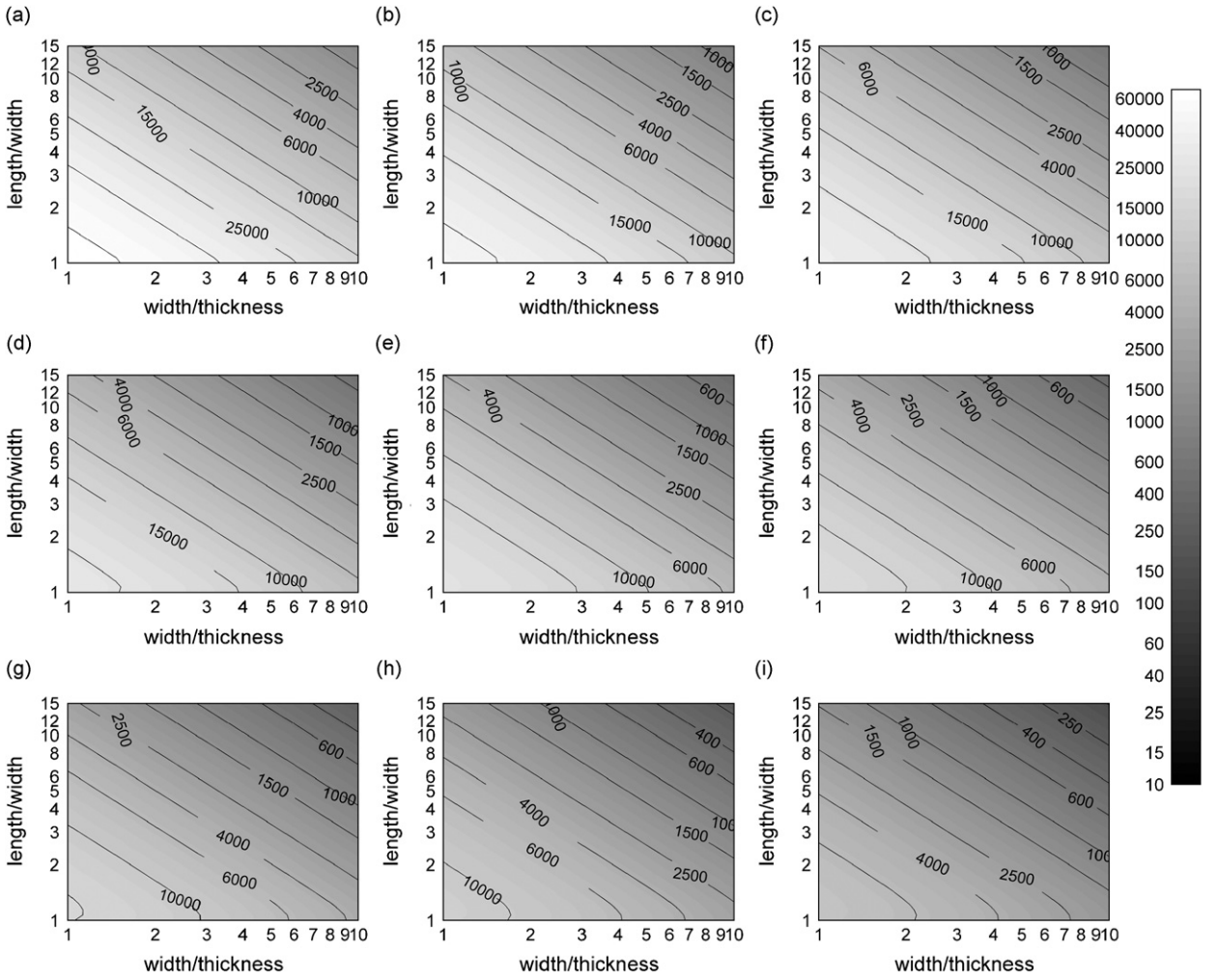

Fig. 3. Frequency of the fundamental flexural mode of a rectangular parallelepiped (Hz), as a function of the sample aspect ratios and the Poisson ratio ν. Constant parameters from Table 1. (a) $\nu = 0.05$, (b) $\nu = 0.1$, (c) $\nu = 0.15$, (d) $\nu = 0.2$, (e) $\nu = 0.25$, (f) $\nu = 0.3$, (g) $\nu = 0.35$, (h) $\nu = 0.4$ and (i) $\nu = 0.45$.

logarithmic axis of Figs. 3–9 and 11–13) were chosen in order to capture the details of the behavior close to aspect ratios equal to 1 (cf. Fig. 10). For each of the $40 \times 30 \times 9 = 10,800$ parameter combinations the resonance frequencies are computed for approximation degrees $n = 6$, 8, 10, 12, 14, 16, 18, 20, 22 and 24 in order to allow studying the asymptotic behavior of the error of the frequencies of interest as n grows to infinity. For this range of values of n, each computation takes about twice as much time as the preceding one. Thus, it takes less to compute the cases $n = 6$, 8, 10, 12, 14, 16, 18, 20 and 22 together than to compute the $n = 24$ case.

In order to estimate the error of the computed resonance frequencies, their relative difference between consecutive values of n, $n = 6$, 8, 10, 12, 14, 16, 18, 20, 22, 24 are computed for each of the $40 \times 30 \times 9$ gridpoints. The maximum absolute value among all gridpoints for each mode is plotted vs. n in Fig. 1. It is evident that the frequencies of the longitudinal vibration mode converge very quickly, leading to a maximum relative difference of about 10^{-10} for the largest values of n. The resonance frequencies of the flexural mode converge more slowly, but fast enough to achieve in the worst case a relative difference smaller than about 10^{-7}. The slowest convergence corresponds to the torsional mode, for which a worst case relative difference of order 2×10^{-6} is achieved. In the case of the flexural mode, convergence is worse for thin square plates. For the torsional mode, the slowest convergence (inside the region of parameters investigated) occurs for thin bars

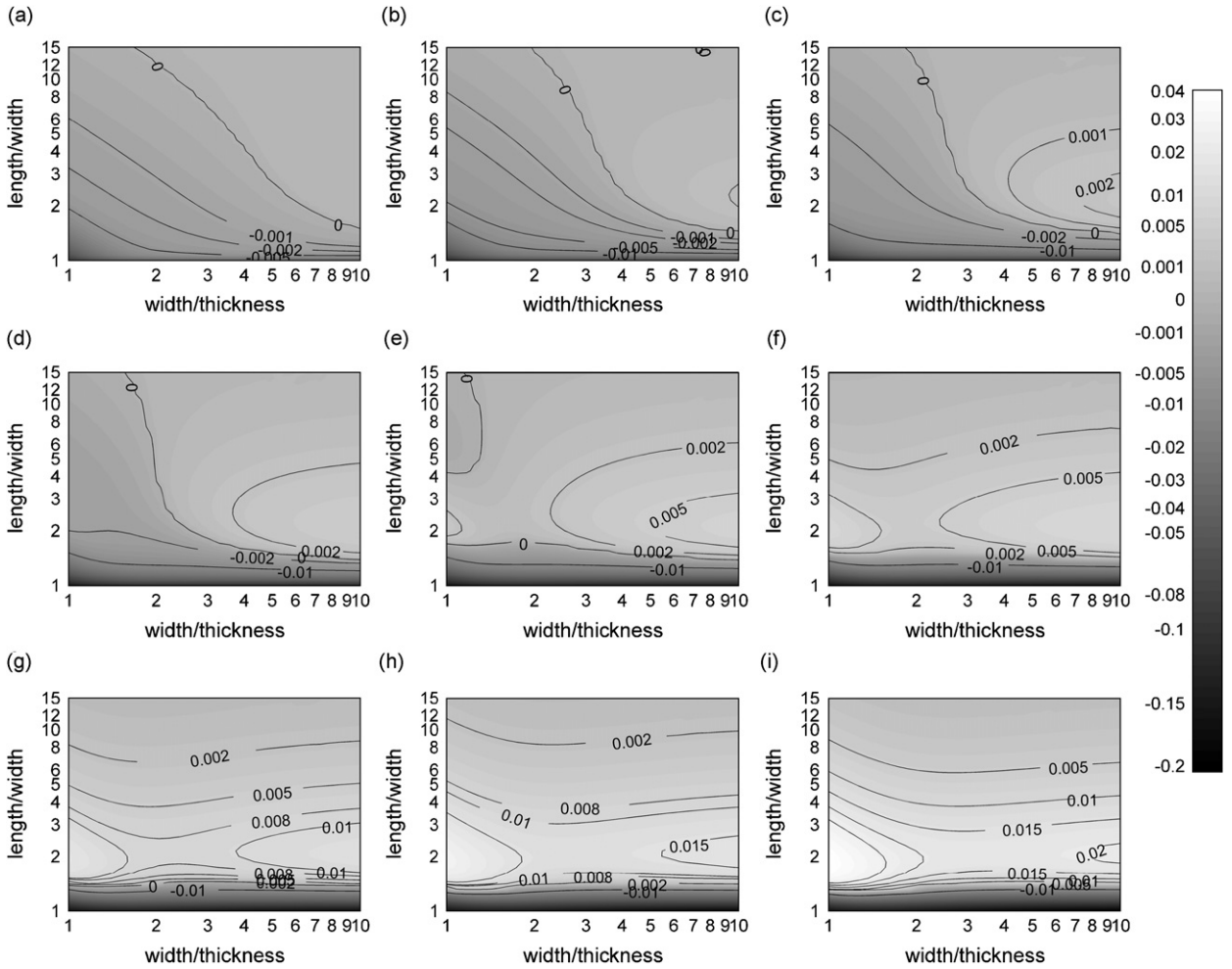

Fig. 4. Relative error of the Young modulus determined from Eq. (9) as a function of the sample aspect ratios, for several Poisson ratio values ν. Constant parameters from Table 1. (a) $\nu = 0.05$, (b) $\nu = 0.1$, (c) $\nu = 0.15$, (d) $\nu = 0.2$, (e) $\nu = 0.25$, (f) $\nu = 0.3$, (g) $\nu = 0.35$, (h) $\nu = 0.4$ and (i) $\nu = 0.45$.

of length-to-width ratio about 8. Finally, the slowest convergence for the longitudinal mode occurs for square plates of any width-to-thickness ratio.

The expected asymptotic behavior of the resonance frequency for any given computational gridpoint is given by

$$\phi_n \sim \phi + \frac{C}{n^m}, \tag{8}$$

where ϕ stands for the extrapolated true frequency of the resonance mode under consideration and ϕ_n is the frequency computed for the given maximum approximation degree n. The exponent m is determined by the smoothness of the corresponding eigenmode. An example of the validity of such an asymptotic expansion is shown in Fig. 2 for length-to-width equal to 5, width-to-thickness equal to 10 and Poisson ratio equal to 0.3. In this case the computations were performed for maximum degrees n from 6 to 34. The asymptotic expansion provides a way to improve the accuracy of the computed resonance frequencies, provided the results for several values of n are available. The main idea is to fit ϕ, C and m in Eq. (8) in such a way that they minimize the difference against the computed ϕ_n, $n = n_1, n_2, \ldots, n_k$. The value for ϕ thus obtained is the improved estimate of the resonance frequency. The accuracy improvement can be substantial, at the price that the accuracy of the improved estimate itself is difficult to assess.

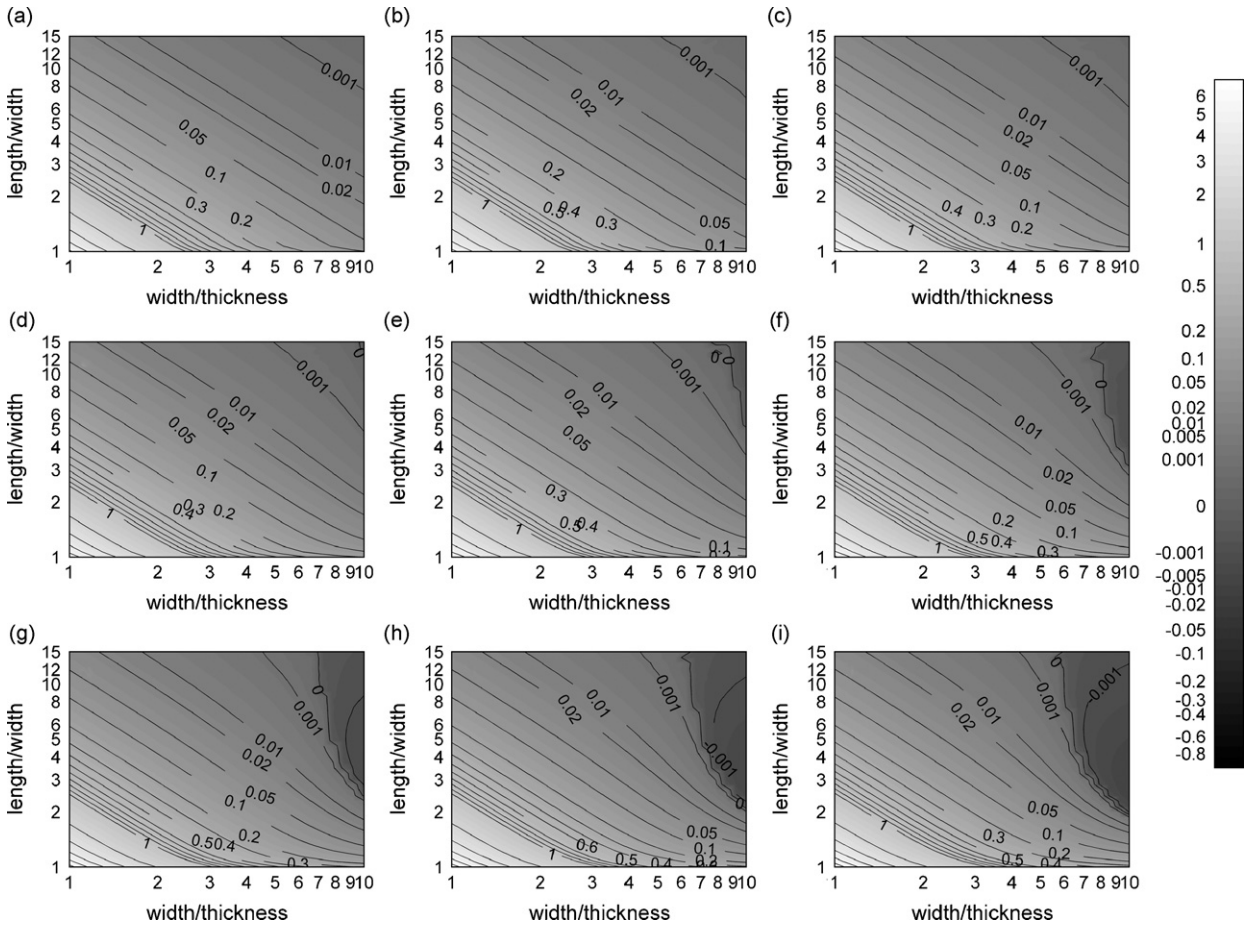

Fig. 5. Correction factor for the Young modulus, as in Eq. (10). Shown is $T_1 - 1$. Constant parameters from Table 1. (a) $\nu = 0.05$, (b) $\nu = 0.1$, (c) $\nu = 0.15$, (d) $\nu = 0.2$, (e) $\nu = 0.25$, (f) $\nu = 0.3$, (g) $\nu = 0.35$, (h) $\nu = 0.4$ and (i) $\nu = 0.45$.

For the computational grid of $40 \times 30 \times 9$ aspect and Poisson ratios the worst case relative accuracy for the longitudinal and flexural resonance modes was already much better than 10^{-6} for $n = 24$. In the case of the torsional resonance mode the worst case relative accuracy of the $n = 24$ computation was estimated in 2×10^{-6}. The estimated relative error of the improved estimate based on Eq. (8) is much smaller.

This evidence suggests that in all cases presented here the relative error of the resonance frequencies is smaller than about 10^{-6}. As with standard means for measuring lengths and frequencies it would be very difficult to perform measurements with errors less than about 0.1 percent, we consider that the estimated 0.0001 percent error is more than enough to justify our evaluation of the standard formulae. Once the resonance frequencies are obtained, the corresponding values of the elastic moduli (according to the standard expressions included for instance in the ASTM standards) are computed and compared to the true moduli (known for each λ and Poisson ratio). In this way, the suitability of the different expressions presented in the literature is assessed for the whole range of geometries and Poisson ratios investigated.

3.1. Flexural mode

To start the analysis, we present in Fig. 3 the dependence of the frequency of the fundamental flexural mode $f_{F,1}$ as a function of the geometrical parameters, for several values of the Poisson ratio. Observe that the axes in the figure are logarithmically spaced, and that the level curves are approximately straight lines of slope -1. This means that for given Poisson ratio and sample length L_x, the frequency depends almost exclusively on the L_x/L_z ratio. The standard expression used in the mechanical resonance techniques to determine the

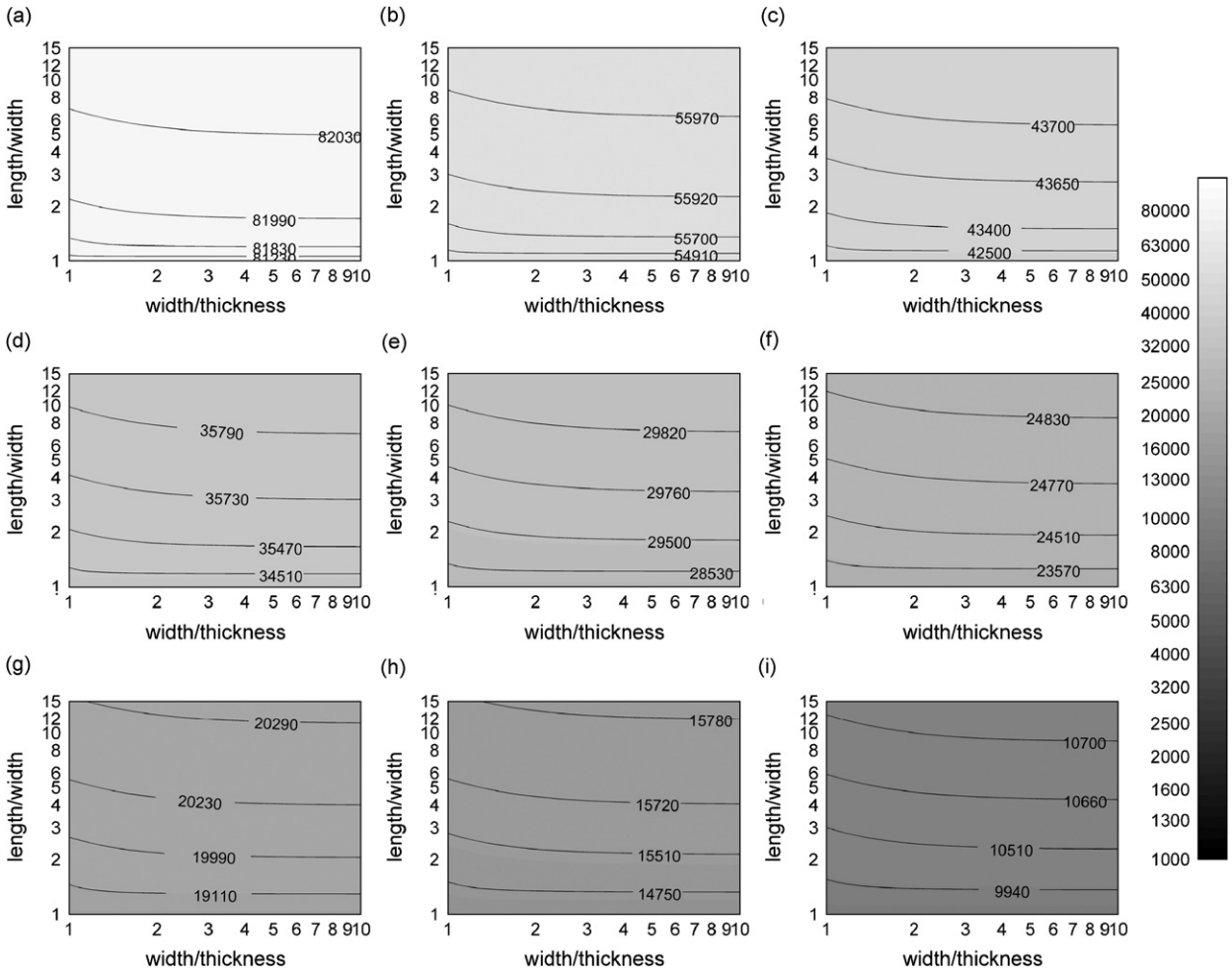

Fig. 6. Frequency of the fundamental longitudinal vibration mode of a rectangular parallelepiped (Hz), as a function of the sample aspect ratios and the Poisson ratio ν. Constant parameters from Table 1. (a) $\nu = 0.05$, (b) $\nu = 0.1$, (c) $\nu = 0.15$, (d) $\nu = 0.2$, (e) $\nu = 0.25$, (f) $\nu = 0.3$, (g) $\nu = 0.35$, (h) $\nu = 0.4$ and (i) $\nu = 0.45$.

Young modulus from the measured frequency is (see [11], and ASTM Standards E1875-00e1, E1876-07, C1548-02 (2007) [1–3])

$$E = 0.9465\rho f_{F,1}^2 L_x^2 \left(\frac{L_x}{L_z}\right)^2 T_1, \tag{9}$$

where T_1 is a factor that takes into account the finite thickness of the bar and the Poisson ratio:

$$T_1 = T_1((L_z/L_x)^2, \nu) = 1 + 6.585(1 + 0.0752\nu + 0.8109\nu^2)\left(\frac{L_z}{L_x}\right)^2 - 0.868\left(\frac{L_z}{L_x}\right)^4 - \left(\frac{8.340(1 + 0.2023\nu + 2.173\nu^2)(L_z/L_x)^4}{1 + 6.338(1 + 0.1408\nu + 1.536\nu^2)(L_z/L_x)^2}\right). \tag{10}$$

For long and thin samples (small L_z/L_x ratio) the correction is small, and can be well approximated by

$$T_1 = 1 + 6.585(L_z/L_x)^2. \tag{11}$$

The general form of the correction factor coincides with the qualitative observations from Fig. 3. The overall relative error of the expression for the Young modulus given by Eqs. (9) and (10) is represented in Fig. 4. It is

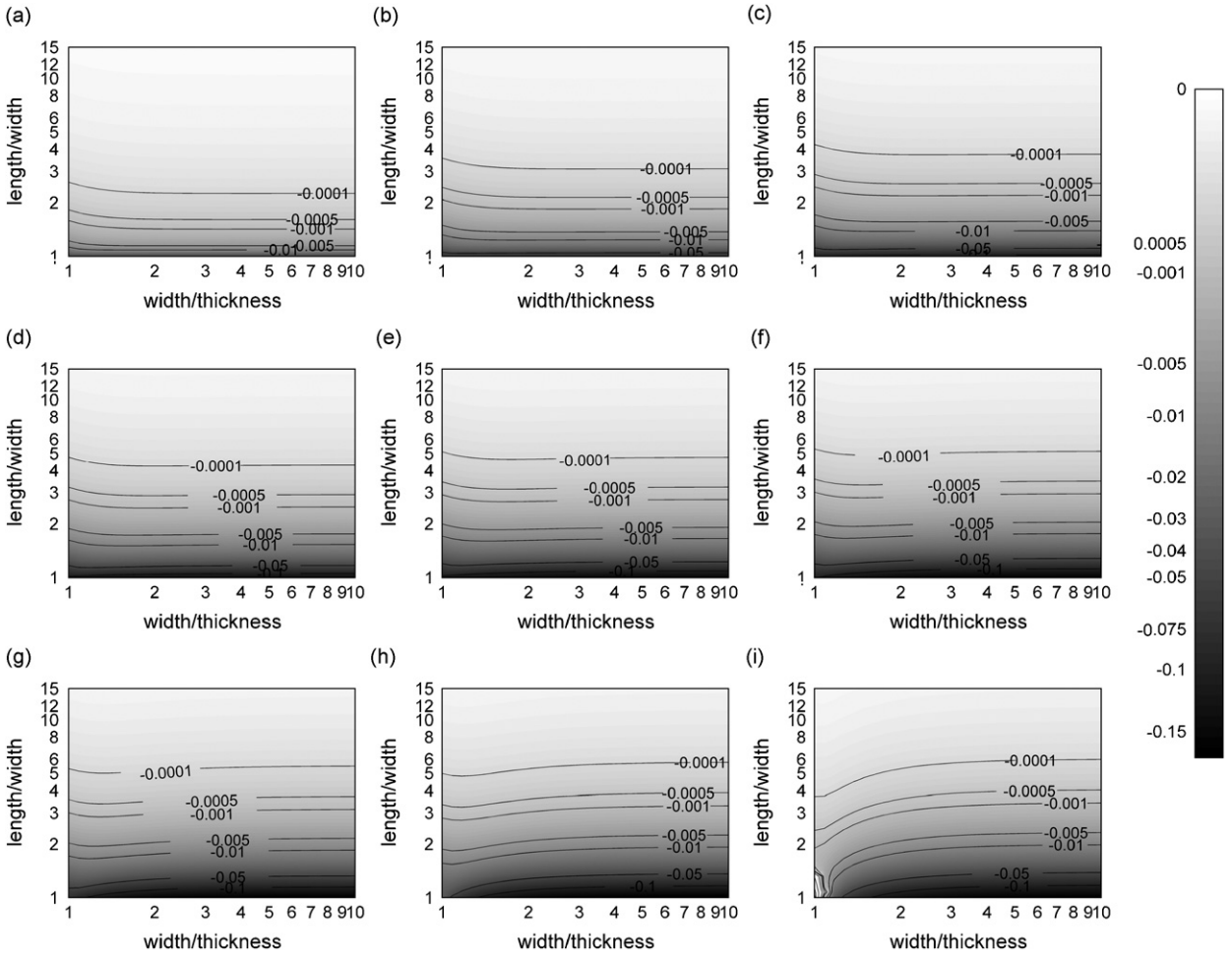

Fig. 7. Relative error of the Young modulus determined from Eq. (12) as a function of the sample aspect ratios, for several Poisson ratio ν values. (a) $\nu = 0.05$, (b) $\nu = 0.1$, (c) $\nu = 0.15$, (d) $\nu = 0.2$, (e) $\nu = 0.25$, (f) $\nu = 0.3$, (g) $\nu = 0.35$, (h) $\nu = 0.4$ and (i) $\nu = 0.45$.

clear from the data that for Poisson ratios smaller than about 0.35, if the length-to-width ratio of the sample is larger than about 2, the errors involved in the use of Eqs. (9) and (10) are smaller than 1 percent. The errors are large if the length-to-width ratio is close to 1, for all thickness values. This is produced by the inability of the correction factor $T_1(L_z/L_x, \nu)$ to capture the dependence on the L_x/L_y ratio for length-to-width ratios close to 1. The correct correction factor (from the numerical computations) is shown in Fig. 5, where the exact $T_1 - 1$ is displayed. It is evident that the behavior at small L_x/L_y, or at large L_y/L_z, does not follow the main trend which could be well represented by a function of L_z/L_x, and is instead a function of the two variables. It is perhaps worth noticing that for long and thin samples (small L_z/L_x) the simplified expression provided by Eq. (11) is not only much simpler to use because no iteration is required, but can also be more accurate than the full correction given by Eq. (10).

3.2. Longitudinal mode

A similar analysis is presented here for the frequency of the fundamental longitudinal vibration mode, which can be used to determine the Young modulus. From Fig. 6, it can be seen that this frequency is essentially dependent on the Poisson ratio, and depends only slightly on the aspect ratios (again, for fixed length L_x and Lamé parameter λ). The approximate expressions that relate this frequency $f_{L,1}$ to the Young

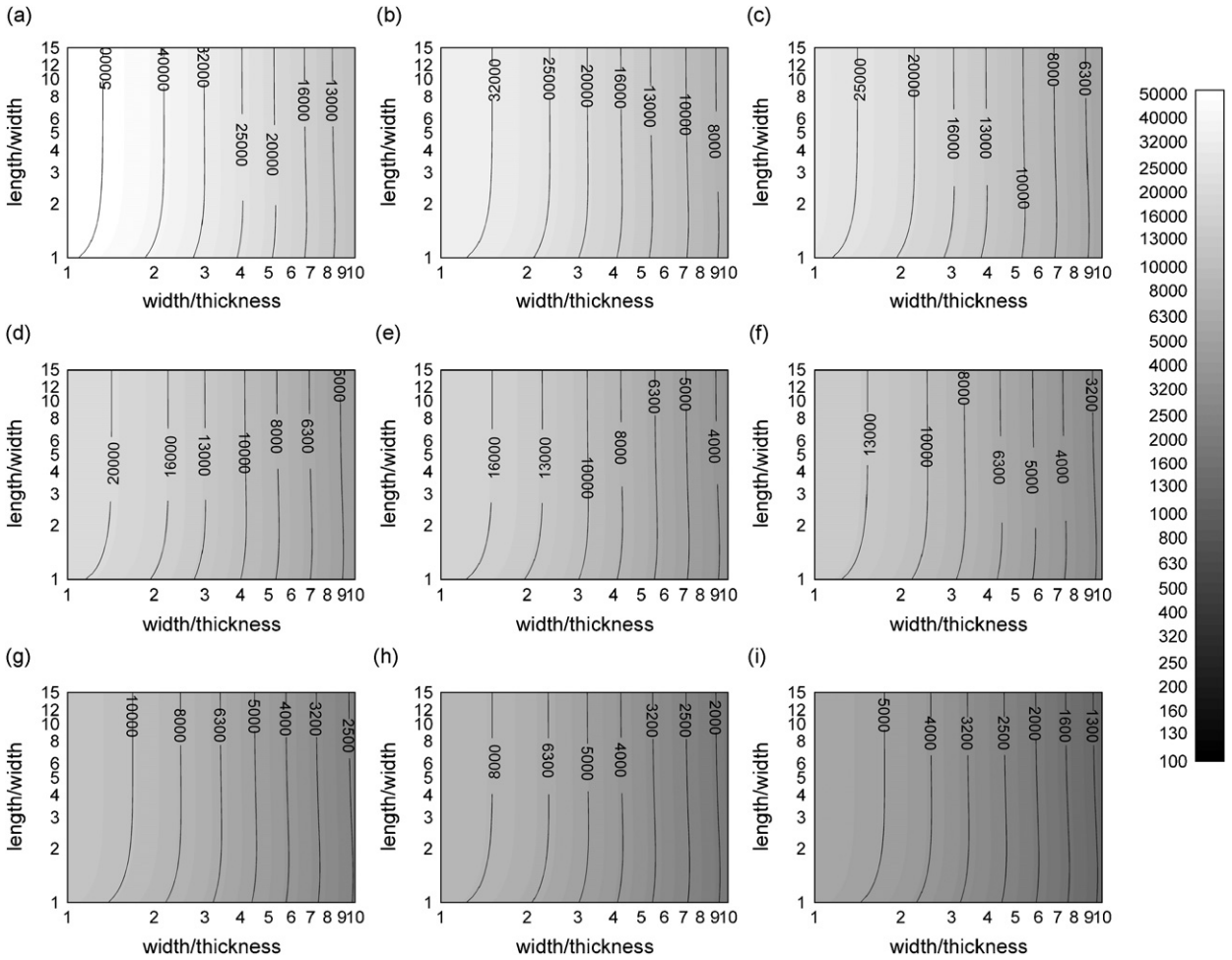

Fig. 8. Frequency of the fundamental torsional mode of a rectangular parallelepiped (Hz) as a function of the sample aspect ratios and the Poisson ratio ν. Constant parameters from Table 1. (a) $\nu = 0.05$, (b) $\nu = 0.1$, (c) $\nu = 0.15$, (d) $\nu = 0.2$, (e) $\nu = 0.25$, (f) $\nu = 0.3$, (g) $\nu = 0.35$, (h) $\nu = 0.4$ and (i) $\nu = 0.45$.

modulus are from [11]:

$$E = 4\rho L_x^2 f_{L,1}^2 \frac{1}{K}. \tag{12}$$

K is a correction factor given by

$$K = 1 - \frac{\pi^2 \nu^2 D^2}{8L_x^2}, \tag{13}$$

where D is an effective sample diameter computed as

$$D^2 = \tfrac{2}{3}(L_y^2 + L_z^2). \tag{14}$$

Fig. 7 shows the comparison between the exact Young modulus, and the one computed from Eq. (12). It is clear that the overall quality of the approximation is quite good, with errors smaller that 0.1 percent for length-to-width ratios larger than 3. Errors increase as the length-to-width ratio diminishes, and also when the Poisson ratio increases. It is perhaps worth mentioning that in spite of the concern expressed in [11], the accuracy of this expression for non-square cross sections is as good as it is for square ones.

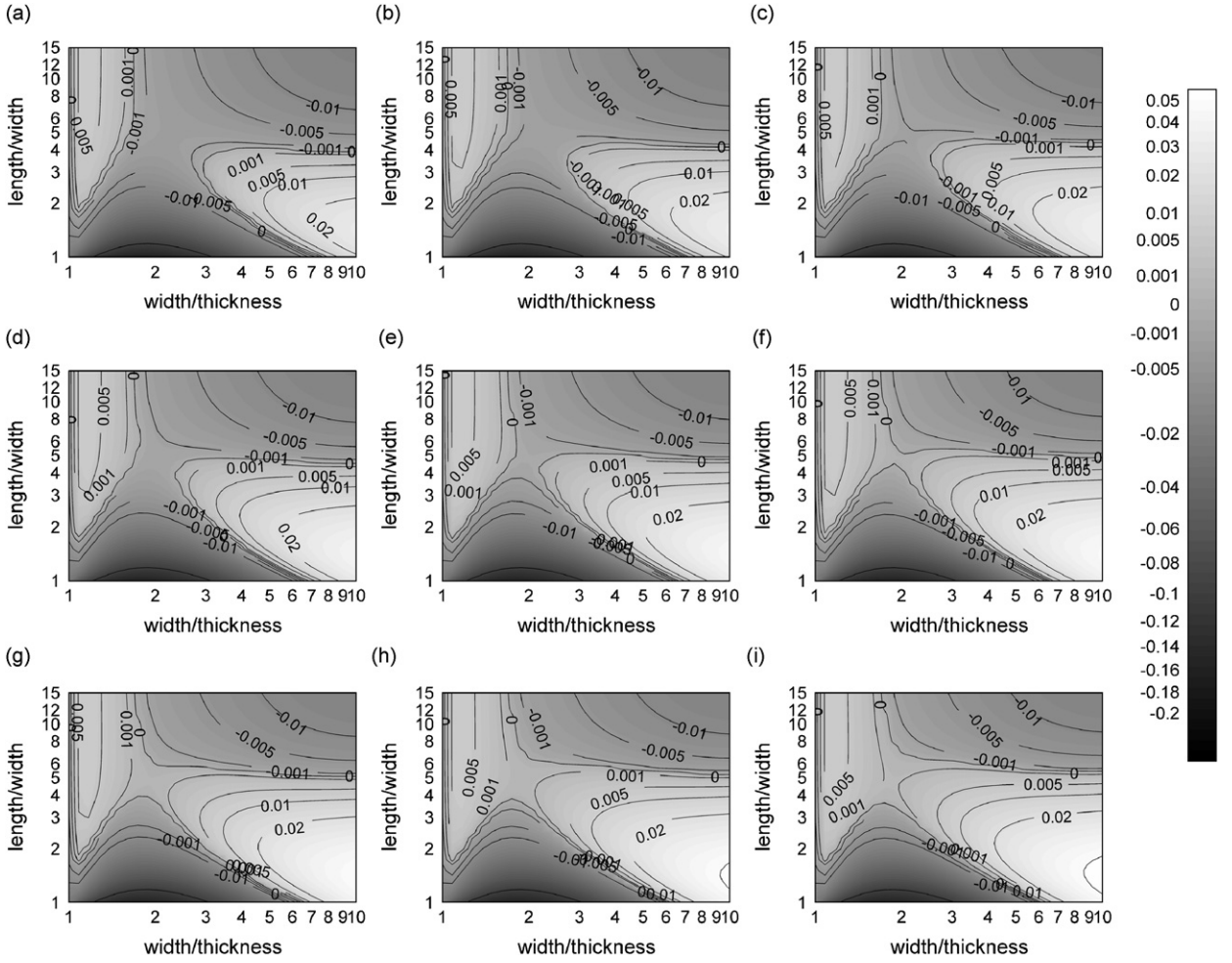

Fig. 9. Relative error of the shear modulus determined from Eq. (15), as a function of the sample aspect ratio, and for several Poisson ratio values. (a) $\nu = 0.05$, (b) $\nu = 0.1$, (c) $\nu = 0.15$, (d) $\nu = 0.2$, (e) $\nu = 0.25$, (f) $\nu = 0.3$, (g) $\nu = 0.35$, (h) $\nu = 0.4$ and (i) $\nu = 0.45$.

3.3. Torsional mode

The frequency of the fundamental torsional mode as a function of the geometrical parameters and the Poisson ratio is shown in Fig. 8. It is evident that the main dependence of the frequency (for fixed length, density ρ and λ) is on the width/thickness ratio.

In the impulse excitation of vibration technique this resonance frequency is used to determine the shear modulus $G = \mu$. For rectangular bars, there are a couple of standard approaches, based on theoretical and experimental evidence gathered in the sixties [10–12]. These are reflected for current practice in the ASTM standards E1876-07, C1548-02 (2007), E1876-01, E1875-00e1, etc.

The expression recommended in ASTM E1876-01, ASTM E1875-00e1, ASTM C1548-02 (2007), is based on [12]

$$G = 4\rho L_x^2 f_{T,1}^2 \left(\frac{B}{1+A}\right), \tag{15}$$

where B is a theoretical correction factor given by

$$B = \frac{(L_y/L_z) + (L_z/L_y)}{4(L_z/L_y) - 2.52(L_z/L_y)^2 + 0.21(L_z/L_y)^6}, \tag{16}$$

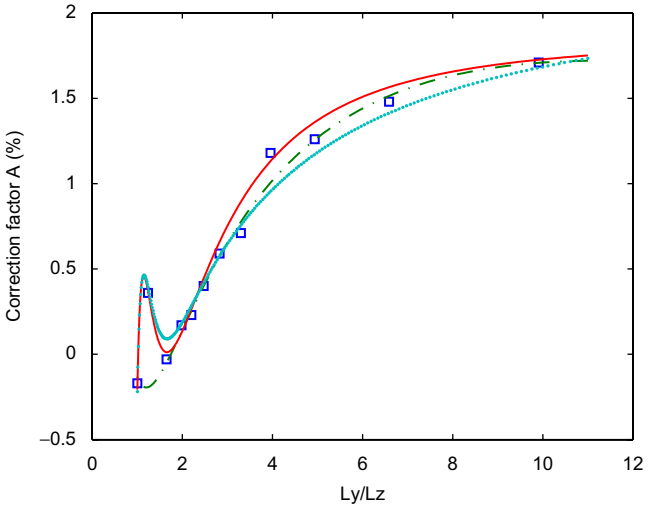

Fig. 10. Correction factor A of Eq. (15), as obtained experimentally by Spinner and Valore [12] (squares), as approximated by Eq. (17) (dash-dot), as computed by the numerical simulations (solid line), and as if Eq. (18) were exact (dots). Sample dimensions are from Ref. [12], $\lambda = 108.4$ GPa is taken from the literature for steel, and $\mu = 82.18$ GPa is obtained numerically as the optimum value to predict the experimental resonance frequencies in [12].

and A is an empirical correction factor dependent on the width-to-thickness ratio:

$$A = \frac{0.5062 - 0.8776(L_y/L_z) + 0.3504(L_y/L_z)^2 - 0.0078(L_y/L_z)^3}{12.03(L_y/L_z) + 9.892(L_y/L_z)^2}. \tag{17}$$

In the current revision of ASTM standard E1876, E1876-2007, the correction factor was changed to favor the analytical expressions from [11] instead of the experimental data, to

$$G = 4\rho L_x^2 f_{T,1}^2 R, \tag{18}$$

where the correction factor R is given by

$$R = \frac{1 + \dfrac{L_y^2}{L_z^2}}{4 - 2.521\dfrac{L_z}{L_y}\left(1 - \dfrac{1.991}{e^{\pi L_y/L_z} + 1}\right)}\left(1 + 0.00851\frac{L_y^2}{L_x^2}\right) - 0.060\left(\frac{L_y}{L_x}\right)^{3/2}\left(\frac{L_y}{L_z} - 1\right)^2. \tag{19}$$

No reason is provided for the change, although for this formula there is a claim that it should be accurate to within 0.2 percent for length-to-width ratio larger than 3.3 and width-to-thickness ratio smaller than 10. Otherwise, the stated error is about 1 percent.

The relative error in G obtained using expressions given in Eqs. (15)–(17) is represented in Fig. 9. For length/width ratios larger than about 3, the maximum error is of the order of a 1 percent. The error does not depend too much on the Poisson ratio, and has a somewhat complex structure. For steel samples, for instance, where Poisson ratio is about 0.3, it would be advisable to work with samples with length/width ratio approximately equal to 5, because the error of this formula is very small for width-to-thickness ratios in the range of 3–10. It is also worth noticing that the maximum error involved in using the empirical correction term $1/(1 + A)$ is of the same order (1 percent) as the corrections it introduces.

It is instructive to have a look at the experimental data from Ref. [12] from the numerical simulations perspective. To this end, we set a reasonable value of λ for steel, $\lambda = 108.4$ GPa, and designed an iterative procedure to minimize the error between the experimental frequencies from Table 2 in [12] and the predicted resonance frequencies, as a function of μ. The sample dimensions used were those quoted in [12], and a polynomial basis with $n = 16$ was chosen. The optimum value for G obtained in this way is $G = 82.18$ GPa, very close to the 82.21 GPa obtained by Spinner and Valore. Fig. 10 shows, for these parameters, the predicted

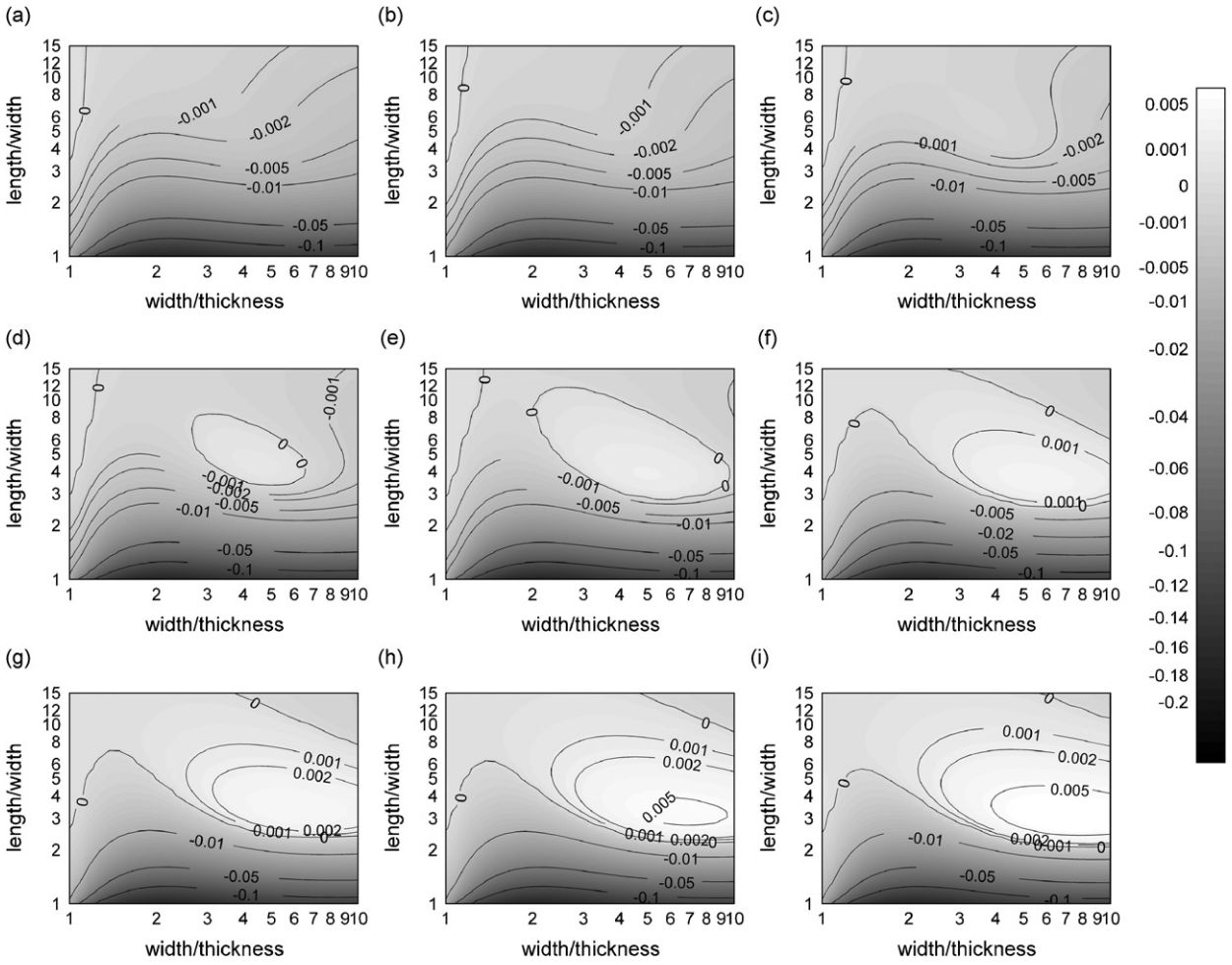

Fig. 11. Relative error of the shear modulus determined from Eq. (18), as a function of the sample aspect ratio, and for several Poisson ratio values. (a) $\nu = 0.05$, (b) $\nu = 0.1$, (c) $\nu = 0.15$, (d) $\nu = 0.2$, (e) $\nu = 0.25$, (f) $\nu = 0.3$, (g) $\nu = 0.35$, (h) $\nu = 0.4$ and (i) $\nu = 0.45$.

'exact' correction factor (thin line), the correction factor computed by Spinner and Valore for their experimental data (represented with squares, taken from Table 3 in [12]), and the standard interpolation given by Eq. (15) (dash-dot curve). It is evident that the very far apart point for width-to-thickness ratio 1.237 is not an outlier, as could be suspected from the interpolation based on Eq. (15). The maximum error introduced by using Eq. (15) in this narrow range of width-to-thickness ratios is of the order of 0.7 percent, but is much larger than the correction itself. For comparison, it is also shown the factor that would be predicted if Eq. (18) was exact (dots). It is clear that the behavior is much closer to the 'real'.

Formulas given by Eqs. (18) and (19), from Ref. [11] and endorsed in the latest revision of ASTM E1876 (2007) standard (but not so in the still current ASTM E1875-00e1, ASTM C1548-02 (2007) standards) do not suffer from this inaccuracy for small width-to-thickness ratios. This can be observed in Fig. 11, where the relative error in the computed shear modulus is represented as a function of the aspect ratios of the sample for several Poisson ratios. The error is concentrated at small length-to-width ratios, and the claims reproduced below Eq. (19) are conceptually valid. However, they are not exactly correct and the answer depends on the width-to-thickness ratio. For instance, for a Poisson ratio equal to 0.3 a length-to-width ratio larger than about 4 is required to achieve an error smaller than 0.2 percent, and this only for width-to-thickness ratio around 2. For Poisson ratios closer to 0.5, and width-to-thickness ratios around 5, the errors are bigger, about 0.5 percent or larger.

Fig. 12 represents the exact correction factor R that should be used in Eq. (18), which is approximated by Eq. (19) for large length-to-width ratios. We see that it is fairly independent on the Poisson ratio, and mainly

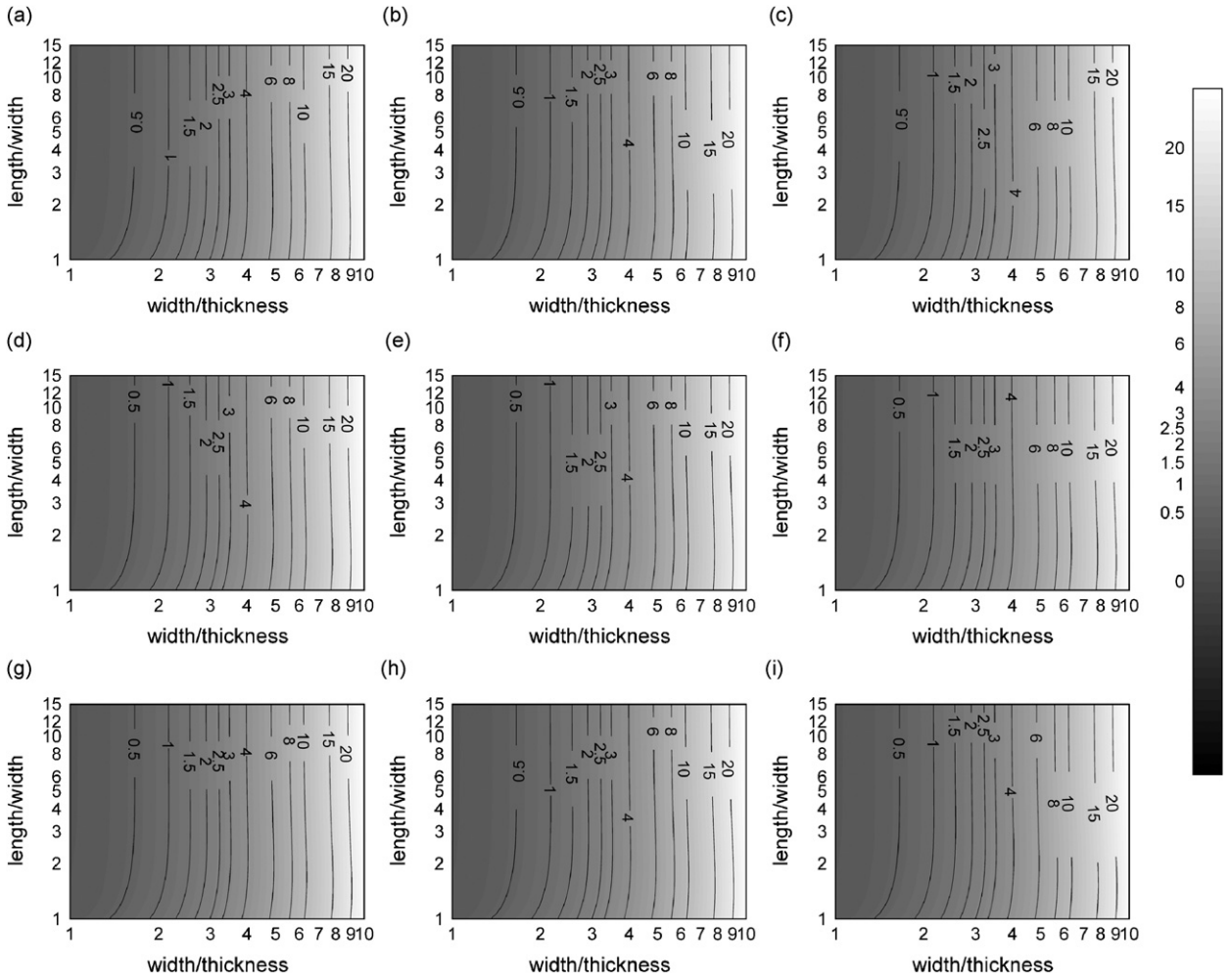

Fig. 12. Exact correction factor in Eq. (18), obtained from the numerical simulations, as a function of the sample aspect ratio, and for several Poisson ratio values. (a) $\nu = 0.05$, (b) $\nu = 0.1$, (c) $\nu = 0.15$, (d) $\nu = 0.2$, (e) $\nu = 0.25$, (f) $\nu = 0.3$, (g) $\nu = 0.35$, (h) $\nu = 0.4$ and (i) $\nu = 0.45$.

dependent on the width-to-thickness ratio. As an observation, the $B/(1+A)$ term in Eqs. (15)–(17) depends only on the width-to-thickness ratio, while the R from Eq. (19) introduces a correction for the slight dependence on the length-to-width ratio (that is not completely successful for small L_x/L_y).

4. Discussion

The results above show that the standard formulae are usually not correct if accuracies better than 1 percent error are sought, unless the aspect ratios are properly chosen in the regions of small error of the parameter space. Eq. (9) for the determination of the Young modulus, and Eq. (18) for the shear modulus should be preferred in general. The exact correction factors for these formulae are represented in Figs. 4 and 11 for the flexural and the torsional resonance modes. Some effort in finding a suitable parameterization for them is worthwhile, and is currently under way.

If these expressions are used, it is better to choose length-to-width ratios as large as 6 or more, for width-to-thickness ratio around 1.5 or 2. The maximum absolute relative error in any of E and G is represented for ease of reference in Fig. 13. The fact that the width-to-thickness ratio should not be too large is good news, because in many cases the magnitude that introduces more experimental error in the result is the thickness of the sample. Of course, the selection of the sample size should take into account the feasibility, the desired

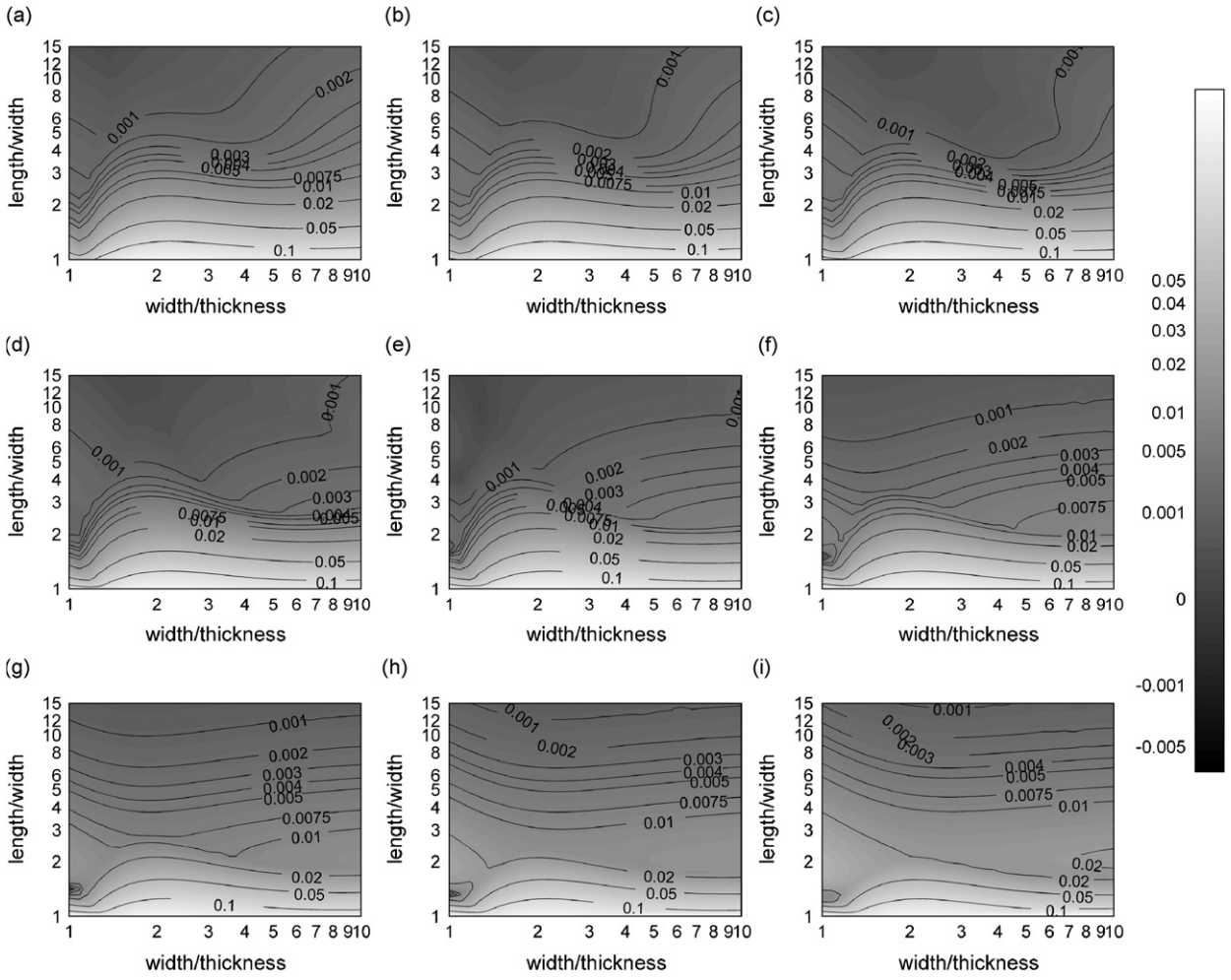

Fig. 13. Maximum absolute relative error in both E and G, computed using Eqs. (9) and (18), respectively, as a function of the sample aspect ratio, and for several Poisson ratio values. (a) $\nu = 0.05$, (b) $\nu = 0.1$, (c) $\nu = 0.15$, (d) $\nu = 0.2$, (e) $\nu = 0.25$, (f) $\nu = 0.3$, (g) $\nu = 0.35$, (h) $\nu = 0.4$ and (i) $\nu = 0.45$.

accuracy, the accuracy achievable in the measurements involved, the fact that the resonance frequencies of interest should be reasonably isolated from others, etc.

If the choice of the sample shape is limited by other reasons, Figs. 4, 7 and 11 can be used to correct the values of the moduli obtained by the standard formulae. A suitable strategy would be to determine the elastic moduli and the Poisson ratio as indicated using Eqs. (12) and (18), and then for the given aspect and Poisson ratios to obtain the relative correction from Figs. 4, 7 and 11. This procedure could be iterated in the case an exceedingly good precision is required, but just only one correction step would be usually enough. For instance, for a steel sample with Poisson ratio equal to 0.3, and length-to-width and width-to-thickness ratios equal to 2 and 5, respectively, the correction for the shear modulus in Fig. 11 is -0.01 (-1 percent). The corrected shear modulus is then 1 percent larger than the one computed from Eq. (18).

5. Conclusions

In this work numerical techniques specifically designed to obtain high precision solutions of the resonance frequencies of elastic parallelepipeds are applied to assess the accuracy of the standard expressions used in the impact excitation of vibration and resonance techniques to determine the elastic moduli of isotropic materials.

Particular attention is paid to the precision of the numerical solutions, and relative errors in the computed frequencies are believed to be smaller than 0.0001 percent for the whole range of length-to-width, width-to-thickness and Poisson ratios analyzed.

The results show that standard formulae are usually not correct if accuracies better than 1 percent error are sought, unless the aspect ratios are chosen such that the error is small enough. Eq. (9) for the determination of the Young modulus, and Eq. (18) for the shear modulus are in general preferable. For these expressions length-to-width ratios as large as 6 or even larger are recommended, together with width-to-thickness ratios around 1.5 or 2. In the case the sample size is limited by other factors, the results shown in the figures reported can be used to apply a simple correction to the value provided by the standard formulae.

References

[1] ASTM Standard E1875-00e1, Standard test method for dynamic Young's modulus, shear modulus, and Poisson's ratio by sonic resonance, ASTM International, West Conshohocken, PA ⟨www.astm.org⟩.
[2] ASTM Standard E1876-07, Standard test method for dynamic Young's modulus, shear modulus, and Poisson's ratio by impulse excitation of vibration, ASTM International, West Conshohocken, PA ⟨www.astm.org⟩.
[3] ASTM Standard C1548-02 (2007), Standard test method for dynamic Young's modulus, shear modulus, and Poisson's ratio of refractory materials by impulse excitation of vibration, ASTM International, West Conshohocken, PA ⟨www.astm.org⟩.
[4] I.G. Ritchie, Improved resonant bar techniques for the measurement of dynamic elastic moduli and a test of the Timoshenko beam theory, *Journal of Sound and Vibration* 31 (4) (1973) 453–468.
[5] F.J. Nieves, F. Gascón, A. Bayón, Natural frequencies and mode shape of flexural vibration of plates: laser interferometry detection and solutions by Ritz's method, *Journal of Sound and Vibration* 278 (2004) 637–655.
[6] M. Radovic, E. Lara-Curzio, L. Riester, Comparison of different experimental techniques for determination of elastic properties of solids, *Materials Science and Engineering A* 368 (2004) 56–70.
[7] R. Holland, Resonant properties of piezoelectric ceramic rectangular parallelepipeds, *Journal of the Acoustical Society of America* 43 (5) (1968) 988–997.
[8] H.H. Demarest, Cube resonance method to determine the elastic constants of solids, *Journal of the Acoustical Society of America* 49 (3, Part 2) (1971) 768–775.
[9] I. Ohno, Free vibration of a rectangular parallelepiped crystal and its application to determination of elastic constants of orthorhombic crystals, *Journal of Physics of the Earth* 24 (1976) 355–378.
[10] G. Equations for computing elastic constants from flexural and torsional resonant frequencies of vibration of prisms and cylinders, *Proceedings of ASTM*, Vol. 45, 1945, pp. 846–865.
[11] S. Spinner, W.E. Tefft, A method for determining mechanical resonance frequencies and for calculating elastic moduli from these frequencies, *Proceedings of ASTM*, 1961, pp. 1221–1238.
[12] S. Spinner, R.C. Valore, Comparison of theoretical and empirical relations between the shear modulus and torsional resonance frequencies for bars of rectangular cross section, *Journal of Research of the National Bureau of Standards* 60(5) (1958) 459–464 (RP2861).
[13] S. Spinner, T.W. Reichard, W.E. Tefft, A comparison of experimental and theoretical relations between Young's modulus and the flexural and longitudinal resonance frequencies of uniform bars, *Journal of Research of the National Bureau of Standards A—Physics and Chemistry* 64A (2) (1960) 147–155.
[14] A. Dimitrov, H. Andrä, E. Schnack, Efficient computation of order and mode of corner singularities in 3D-elasticity, *International Journal for Numerical Methods in Engineering* 52 (2001) 805–827.
[15] J.A. Fromme, A.W. Leissa, Free vibration of the rectangular parallelepiped, *Journal of the Acoustical Society of America* 48 (1, Part 2) (1970) 290–298.
[16] J.R. Hutchinson, S.D. Zillmer, Vibration of a free rectangular parallelepiped, *Journal of Applied Mechanics* 50 (1983) 123–130.
[17] P. Ciarlet, *The Finite Element Method for Elliptic Problems*, in: *Studies in Mathematics and its Applications*, Vol. 4, North-Holland Publishing Company, 1978.